

# Intensification and Optimization of FAME Synthesis via Acid-Catalyzed Esterification Using Central Composite Design (CCD)

Alaaddin M. M. Saeed,\* Shivika Sharma, Saeikh Zaffar Hassan, Atef M. Ghaleb, and Gui-Ping Cao

Cite This: *ACS Omega* 2023, 8, 26206–26217

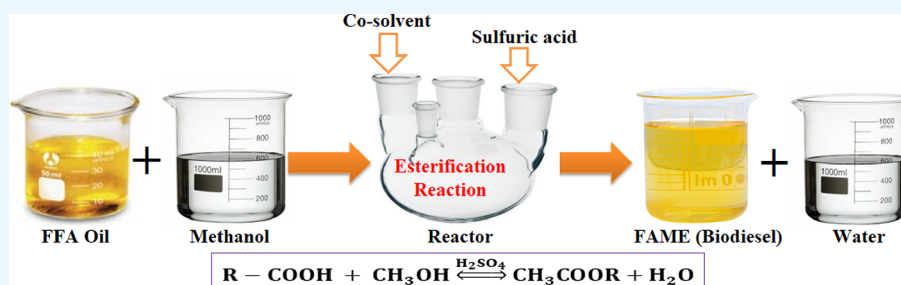
Read Online

ACCESS |

Metrics &amp; More

Article Recommendations

Supporting Information



**ABSTRACT:** The acid-catalyzed pre-treatment esterification process is required for low-cost feedstock with high free fatty acids (FFAs) to avoid the saponification that occurs during alkali-catalyzed transesterification for the production of fatty acid alkyl esters (FAAE). Reverse hydrolysis in acid-catalyzed esterification causes a decrease in fatty acid methyl ester (FAME) yield. Therefore, the esterification process must be intensified. This study aims to develop and optimize a low-temperature intensification process to enhance biodiesel yield and reduce energy consumption. Three intensification systems were studied: co-solvent technique, co-solvent coupled with adsorption of water using molecular sieves, and entrainer-based continuous removal of water. The process variables of esterification reaction in co-solvents without the adsorption system were optimized by using central composite design (CCD). The study showed that the co-solvent without the adsorption system was effective in intensifying the FFA conversion ( $X_{FFA}$ ) at low temperatures, compared to the other two systems, due to the dilution effect at high co-solvent/entrainer amount required for sufficient vapors in the adsorption system. Optimized process variables have achieved 95%  $X_{FFA}$  within 75 min at 55 °C, 20 mL/100 g of oil DEE, 9 MR, 3 wt %  $H_2SO_4$ , and 320–350 RPM in a co-solvent without the adsorption system.

## 1. INTRODUCTION

Biofuels are used worldwide to minimize fossil fuel consumption and as an effort to reduce climate change and global warming. Vegetable oils and animal fats are the two most popular biodiesel feedstock.<sup>1,2</sup> These two renewable feeds containing renewable lipids are the main sources of fatty acid alkyl esters (FAAE),<sup>3</sup> but these are edible and of high cost.<sup>4</sup> As a consequence, the biodiesel derived from these sources is not economically feasible.<sup>5</sup> In order to reduce biodiesel costs, producers use nonedible feedstock such as waste cooking oils and nonedible oils.<sup>6,7</sup>

Used cooking oils typically contain 2–7% free fatty acids (FFAs), animal fats contain 5–30% FFAs, and very low-quality feedstock, such as trap grease, may approach 100% of FFAs. However, to prevent catalyst deactivation, oils used in alkaline trans-esterification reactions should contain no more than 1% FFAs.<sup>3</sup> FFAs and water rapidly react with the catalyst and consume it, and long-chain soaps are formed.<sup>8</sup> Therefore, an acid-catalyzed pre-treatment esterification step is required for high-content FFA feedstock.

Esterification is a reversible type of second-order reaction, in which the yield of alkyl esters decreases as the reaction proceeds because of reverse hydrolysis reaction.<sup>9</sup> Alkyl ester

yield can be increased either by taking one of the reactants in excess,<sup>10</sup> which is generally alcohol, in the case of esterification reaction and/or by continuously removing one of the products from the reaction mixture during the reaction, which can be water. Removal of water can be an effective way to intensify the esterification reaction and enhance the conversion as water causes poisoning to acid catalysts. Several water removal systems like free evaporation, vacuum evacuation, pervaporation, dry gas bubbling,<sup>11</sup> azeotropic reactive distillation,<sup>12,13</sup> stripping of water,<sup>14</sup> and adsorption<sup>3,15</sup> have been suggested in the literature for solvent-free systems. However, they are not suitable when organic solvents are used. Looking for the alternative low-temperature systems suggested by researchers, adsorbents and co-solvent systems have been found. In particular, a co-solvent system has been employed by some

Received: April 11, 2023

Accepted: May 29, 2023

Published: July 14, 2023



researchers in transesterification reactions. It was reported that the highest conversion (97.98%) of biodiesel was obtained by using 20 wt % of co-solvent (acetone), 1:6 M ratio of oil:methanol, and 1.2 wt % calcium aluminate at  $55 \pm 1$  °C for 25 min of reaction time.<sup>16</sup> Methanol and oil phases are completely immiscible in the temperature range of 25 to 60 °C.<sup>17</sup> Also, methanol and oil are insoluble and can result in phase separation<sup>18</sup> and the mass transfer between both the phases affects the reaction rate.<sup>17,19</sup> Therefore, the co-solvent improves the mass transfer between the phases present in the transesterification process by increasing the mutual solubility between reactants, and it is usually easy to be recovered and reused.<sup>20</sup> However, the co-solvent system has not yet been used by researchers in the esterification reaction. In this study, the co-solvent system was used for intensification of the esterification reaction at low temperature. The intensification of esterification of FFAs with methanol at low temperature was under study to improve the yield of alkyl esters using different systems like co-solvents and adsorption of water. When the organic solvent is used as a reaction medium, the selective removal of water is complicated due to the lower boiling point of the solvent compared to water. The methanol used in esterification reaction has a boiling point of 64.7 °C, which is much less than that of water. Adsorbent systems have been employed in biodiesel production by some researchers, Lucena et al.<sup>3</sup> reported that an adsorption system was effective in displacing the equilibrium toward the products in the range from 90.9 to 99.9% after 60 min at 100 °C. The use of the adsorption column for water removal may allow using lower alcohol to FFA molar ratios in biodiesel processing.<sup>15</sup> Therefore, co-solvent and adsorption systems can be used for intensifying the esterification reaction at low temperature.

## 2. MATERIALS AND METHODS

**2.1. Materials.** Methanol dried (GR grade, moisture <0.02%), diethyl ether (DEE-specially dried), acetone (EMPLURA), water (Millipore grade), 3A molecular sieve, and oxalic acid dihydrate (EMPLURA R) were supplied by Merck Life Science Private Ltd., Mumbai. Fisher Scientific India, Mumbai, supplied pure oleic acid, phenolphthalein indicator, sulfuric acid (97% SQ grade), and *n*-hexane (AR grade). Refined sunflower oil (max. 0.1 wt % FFA) was purchased from Adani Wilmar Ltd., India. Potassium hydroxide (extra pure AR) was supplied by Sisco Research Laboratories Pvt., Ltd., Ahmedabad.

**2.2. Central Composite Design (CCD).** The CCD is considered the best method to optimize the experiments with a quantitative independent variable, and its dependent variable can also be measured in quantity. There are two methods available to apply CCD; the first method is rotatable central composite design (RCCD), which has advantages in extrapolating the data points and the optimum points outside the selected range of the independent variable. The second method is face-centered central composite design (FCCD), which efficiently finds the optimum values within the selected range of independent variables. FCCD was selected to observe the effects of various process variables on predicting optimum fatty acid methyl ester (FAME) yield. Two levels and three factors with six center point values were considered for this method; the total number of experiments suggested through this method was 20 batch experiments. The independent variables selected for the optimization study were catalyst (wt %), temperature (°C), and co-solvent (mL/100 g of oil). The

response factor chosen was the FFA conversion ( $X_{\text{FFA}}$ ) yields produced through a sulfuric acid-catalyzed esterification reaction of 50 wt % oleic acid (OA) (mixed as FFA in sunflower oil) with methanol at 320–350 RPM. The actual values and coded levels of the independent variables are listed in Table 1.

**Table 1. CCD of Experiments for 50% OA in Oil**

std order	run	catalyst (wt %)	temperature (°C)	co-solvent (mL/100 g of oil)
1	14	−1.000	−1.000	−1.000
2	20	1.000	−1.000	−1.000
3	17	−1.000	1.000	−1.000
4	7	1.000	1.000	−1.000
5	5	−1.000	−1.000	1.000
6	4	1.000	−1.000	1.000
7	9	−1.000	1.000	1.000
8	3	1.000	1.000	1.000
9	16	−1.000	0.000	0.000
10	1	1.000	0.000	0.000
11	6	0.000	−1.000	0.000
12	18	0.000	1.000	0.000
13	2	0.000	0.000	−1.000
14	13	0.000	0.000	1.000
15	10	0.000	0.000	0.000
16	15	0.000	0.000	0.000
17	19	0.000	0.000	0.000
18	11	0.000	0.000	0.000
19	12	0.000	0.000	0.000
20	8	0.000	0.000	0.000
Reaction parameters		Level (−1)	Level (0)	Level (+1)
catalyst (wt %)		0.5	1.25	2
temperature (°C)		50	60	70
co-solvent (mL/100 g of oil)		20	30	40

Since adding DEE to the system allows to reach up to 70 °C, the temperature is taken in the range of 50 to 70 °C (see the effect of co-solvent on miscibility in Table 2). The catalyst

**Table 2. Effect of Co-Solvent on Miscibility at 6 MR**

reaction mixture	bath temperature (°C)	maximum reaction temperature (°C)
0% FFA oil/0% solvent	85	65 ± 1
50% FFA oil/0% solvent	85	65 ± 1
50% FFA oil/50% acetone	85	67 ± 1
50% FFA oil/50% DEE	85	70 ± 1

amount is taken in the range of 0.5 to 2 wt % based on the OA amount for all the reactions. The volume percent (vol %) of DEE for better  $X_{\text{FFA}}$  is dependent on the molar ratio (MR) of the methanol in the reaction system. However, the absolute amount of DEE required is the same for both six and nine MR reactions (see Section 4.4). Therefore, MR is fixed as 6 based on the OA amount for all the reactions. DEE is taken in the range of 20 to 60 mL/100 g of oil because a high amount of DEE has shown a negative effect on  $X_{\text{FFA}}$  (see Co-solvent DEE

section). The batch reactions for each experiment were conducted randomly to minimize systematic error.

**2.3. Selection of Co-Solvent.** Various co-solvents were suggested by many researchers for the production of biodiesel, such as tetrahydrofuran (THF), DEE, acetone, and acetonitrile, as listed in Table S1.<sup>21</sup> OA is insoluble in acetonitrile, hexane, and pentane.<sup>21</sup> Therefore, these solvents are of no use in esterification reaction as they will be unable to make the reaction mixture homogeneous. Methanol, FAME, OA, and water are easily dissolved in acetone and THF. Therefore, the esterification of oil with methanol to produce FAME can be performed entirely in the homogeneous phase with these co-solvents. Nevertheless, THF tends to form peroxide on storage and has various toxicological effects on health and the environment.<sup>19</sup> Besides, the recuperation of this co-solvent is very difficult.<sup>20</sup> Therefore, THF is not considered in this study. Usually, the ethers are considered as good as co-solvents because they contain the balance of polar and nonpolar entities required to lower the interfacial surface tension between methanol and vegetable oil.<sup>20</sup> Methanol and OA are easily dissolved in DEE and can generate an oil-rich single-phase system so that all reactions are taking place in the same phase, allowing better contact between the reactants and hence faster reactions. Therefore, DEE and acetone are selected in this study as co-solvents to check their effectiveness in the case of esterification reaction of FFA with methanol.

### 3. EXPERIMENTAL PROCEDURE

The schematic diagrams of the experimental setup for esterification reaction with co-solvent and without co-solvent systems are shown in Figures 1 and 2, respectively.

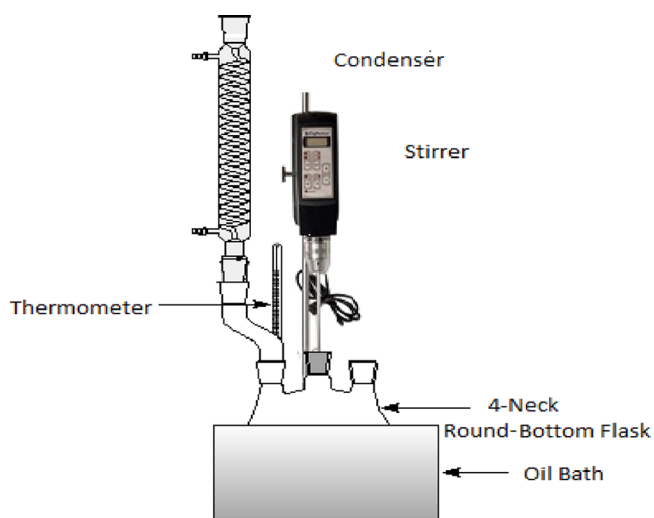


**Figure 1.** Schematic diagram of the experimental setup for esterification reaction without co-solvent.

OA is mixed as FFA with refined sunflower oil in a 1 L four-neck round-bottom flask connected to a helical reflux condenser. The flask is placed in a water bath and heated to set the reaction temperature. Methanol is then added to the reaction mixture according to the MR of methanol to OA. A measured amount of co-solvent is added in accordance with the vol % of methanol in a 1 L four-neck round-bottom flask before reaching the set point temperature (in the case of the co-solvent system only). Once the temperature reaches set 1,

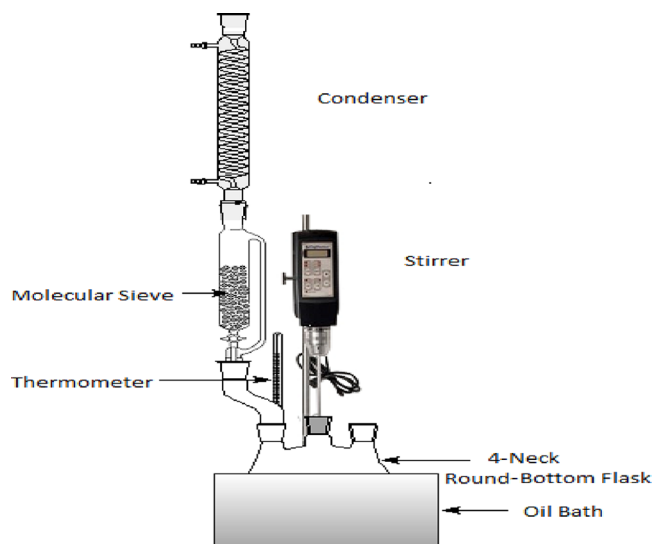


**Figure 2.** Schematic diagram of the experimental setup for esterification reaction with co-solvent.

the calculated amount of sulfuric acid (solution in methanol) is added into the flask. The point of mixing of the catalyst is taken as the starting time of reaction. Throughout the reaction, the mixture is stirred at 420–450 RPM. Samples (3–4 mL each) are withdrawn for analysis at different intervals and transferred in vials. 2 mL of *n*-hexane (cold) is mixed with a sample to stop the reaction, sulfuric acid is separated, and then 4–5 mL of cold Millipore water is added. The aqueous and organic layers are separated by vigorous mixing followed by centrifuging for 5 min (4000 RPM). A pipette is used to remove the aqueous layer. Again, 5 mL of water is added to the organic layer and the mixture is centrifuged to remove traces of sulfuric acid into the water. The organic layer is then transferred to a 10 mL vial kept in a hot air oven at 110 °C to remove water, methanol, and *n*-hexane.

#### 3.1. Experimental Analysis and Data Interpretation.

To determine the wt % of FFA (i.e., OA), samples are titrated with standard 0.05 and 0.025 N potassium hydroxide solution using phenolphthalein as an indicator. The formula for FFA percentage calculation is as follows:

$$\text{FFA}\% = \frac{V \times N_{\text{KOH}} \times 282}{10 \times \text{weight of sample}} \quad (1)$$

where  $V$  is the volume of potassium hydroxide solution consumed and  $N_{\text{KOH}}$  is the normality of potassium hydroxide solution used in the titration. For the calculation conversion percentage of FFA into FAME, the following formula is used.

$$\text{conversion}\% = \frac{\text{initial}\% \text{ of FFA} - \text{final}\% \text{ of FFA}}{\text{initial}\% \text{ of FFA}} \times 10 \quad (2)$$

Design-Expert software (12th version) is used to generate DOE, analysis of results, regression models, and interpretation of the optimization.

## 4. RESULTS AND DISCUSSION

**4.1. No Co-Solvent System.** **4.1.1. Effect of MR.** The methanol-to-OA MR significantly increased  $X_{\text{FFA}}$  as it shifted the reaction to the forward direction. The effect of MR on esterification (without co-solvent or entrainer) at 40 °C was

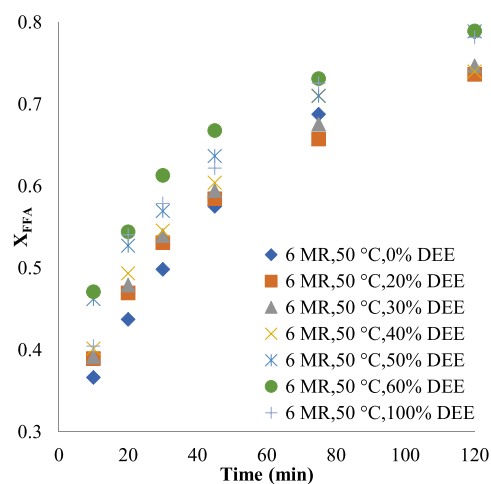


Figure 3. Effects of DEE added in different vol % at 50 °C and 6 MR.

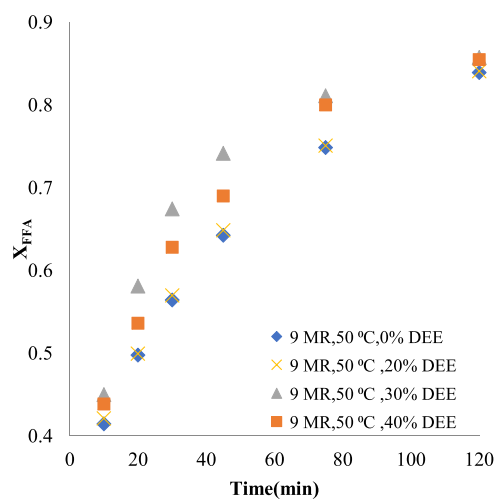


Figure 6. Effects of DEE added in different vol % at 50 °C and 9 MR.

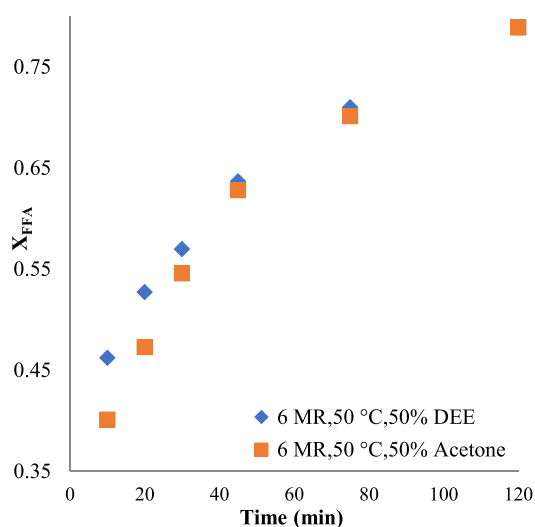


Figure 4. Comparison between DEE and acetone at 50 °C and 6 MR.

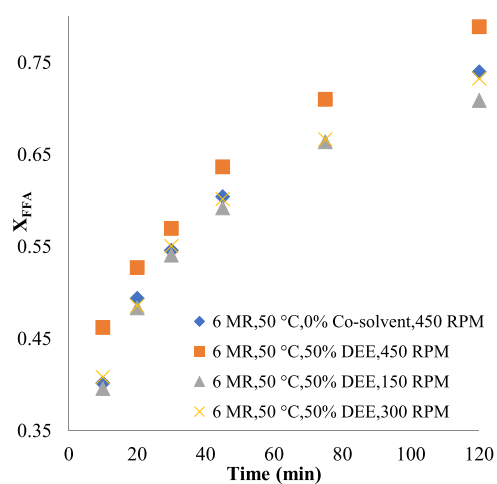


Figure 7. Effect of agitation rate on  $X_{FFA}$  for 50 vol % DEE compared to no co-solvent.

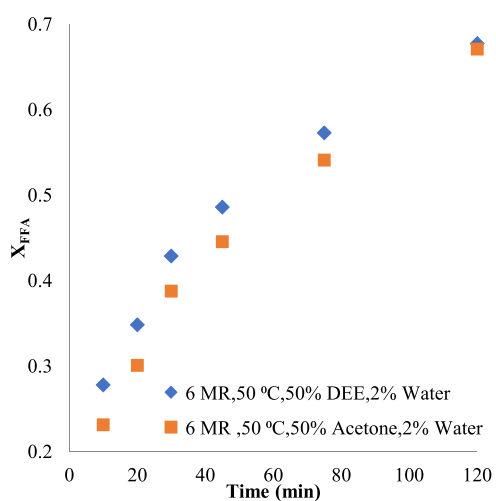


Figure 5. Susceptibility of 50 vol % co-solvent systems for water.

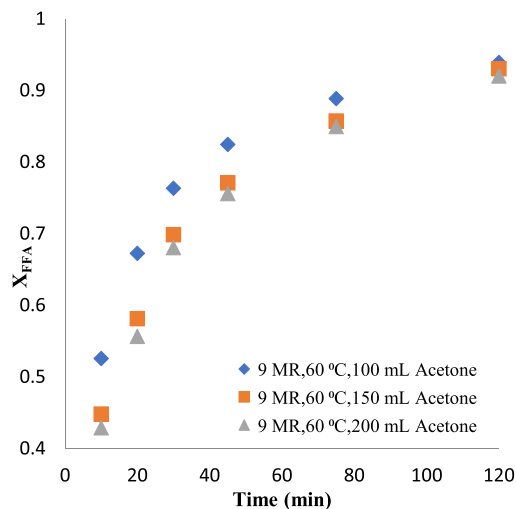
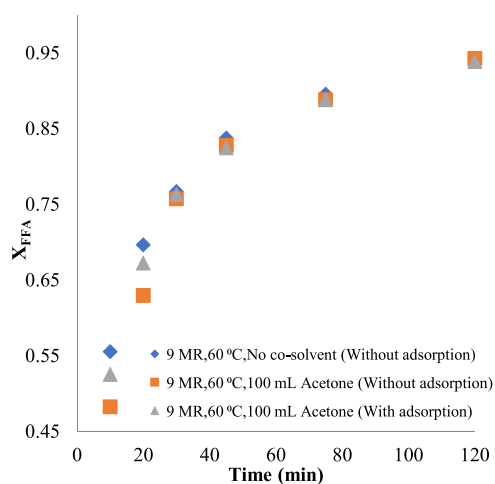


Figure 8. Acetone system: adsorption of water using molecular sieves.

studied, as shown in Figure S1.  $X_{FFA}$  increased rapidly in the beginning and later slowed down, approaching equilibrium because the esterification of FFA is a reversible system.<sup>9</sup>  $X_{FFA}$

also increased with MR due to better successful collisions among reactant molecules.

4.1.2. Effect of Temperature. Temperature is a significant parameter in reactions as it controls the reaction kinetics and



**Figure 9.** Acetone system: adsorption of water using a molecular sieve.

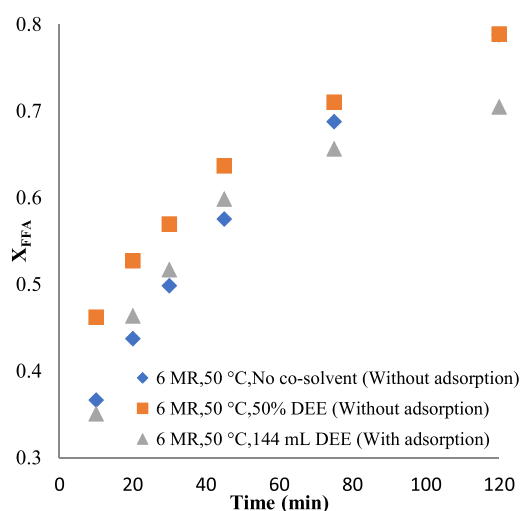


**Figure 10.** DEE system: adsorption of water using molecular sieves.

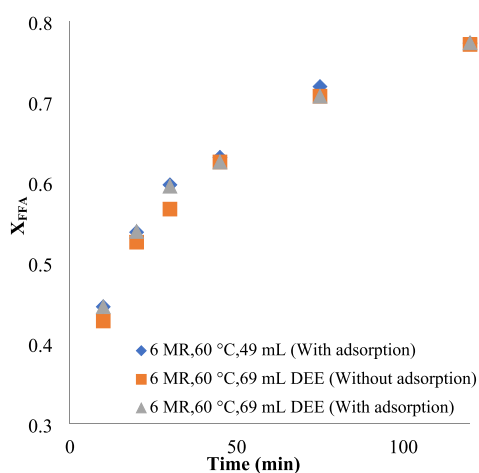


**Figure 11.** DEE system: adsorption of water using molecular sieves.

diffusion rates of reactants and products.<sup>22,23</sup> The effect of temperature on  $X_{\text{FFA}}$  at 9 MR in the absence of any co-solvent is depicted in Figure S2.  $X_{\text{FFA}}$  increased by 7% in the first 10 min and increased by 14% approximately after 75 min on temperature rise from 40 to 50 °C. Additionally,  $X_{\text{FFA}}$

increased when the temperature rose from 50 to 60 °C, and this is due to an increase in successful collisions between reactant molecules with temperature. The activation energy of the reactant molecules was easy at a high temperature, which caused an increase in the rate of reaction.<sup>24</sup> Hence, an increase in temperature can be an effective way to increase  $X_{\text{FFA}}$ .

**4.2. Co-Solvent System.** **4.2.1. Co-Solvent DEE.** Figure 3 shows  $X_{\text{FFA}}$  at 50 °C and 6 MR, using DEE as a co-solvent in different proportions, based on the vol % of methanol. Up to 50–60 vol %, DEE resulted in high  $X_{\text{FFA}}$  and further addition of DEE showed no improvement in  $X_{\text{FFA}}$ . In the case of 60 vol % DEE,  $X_{\text{FFA}}$  was increased from 36.4 to 47.1% in the first 10 min and from 68.7 to 73.3% within 75 min compared to no co-solvent.  $X_{\text{FFA}}$  reached 79% after 120 min for both the no co-solvent and 50–60 vol % DEE systems.

**4.2.2. Co-Solvent Acetone.** The effect of acetone at 50 °C and 6 MR on  $X_{\text{FFA}}$  is depicted in Figure S3. The acetone amount was varied from 30 to 50 vol %, and the results were compared with the experiments without co-solvent. After the addition of acetone,  $X_{\text{FFA}}$  improved. Moreover, there was an increase in  $X_{\text{FFA}}$  at the initial phase of the reaction, but within 75 min,  $X_{\text{FFA}}$  reached the same value as  $X_{\text{FFA}}$  without co-solvent.

The comparison of DEE and acetone at 6 MR and 50 °C is shown in Figure 4. At equal vol % of co-solvent, DEE resulted in a high conversion rate in the initial phase of the reaction whereas the  $X_{\text{FFA}}$  was the same for both the co-solvents after 45 min of reaction. This is because water is soluble in acetone and insoluble in DEE. The solubility of water in acetone causes the poisoning of a sulfuric acid catalyst, resulting in lower  $X_{\text{FFA}}$  at the initial stage.

**4.3. Effect of Water.** In the case of co-solvents, it was observed that  $X_{\text{FFA}}$  reached the same value as in the case of no co-solvent after 120 min of reaction time (see Figures 3 and 4, and Figure S3). Equilibrium  $X_{\text{FFA}}$  for the reaction condition of 50 °C and 6 MR is calculated from the data of Hassan and Vinjamur<sup>9</sup> and found to be 89.9%. The maximum  $X_{\text{FFA}}$  obtained for both the systems, co-solvents and no co-solvent, is ~79% at 50 °C and 6 MR, which is significantly lesser than the calculated equilibrium conversion (89.9%). Therefore, the poisoning of the acid catalyst by water at the later stage of reaction could be the reason for attaining the same  $X_{\text{FFA}}$  after 120 min. To check the effectiveness of co-solvents in hindering the poisoning effect of water, 2 wt % water was added in the reaction mixture initially and the results are compared with no co-solvent experiments, as shown in Figures S4 and S5. Figure S4 shows that  $X_{\text{FFA}}$  decreased drastically when 2 wt % water is added to the acetone system. No differences in  $X_{\text{FFA}}$  were found between 50 vol % acetone and no co-solvent experiments throughout the reaction in the presence of 2 wt % water. Acetone is not effective in improving the  $X_{\text{FFA}}$  in the presence of water because water is soluble in acetone and results in the catalyst's poisoning. In Figure S5, the addition of 2 wt % water also decreased  $X_{\text{FFA}}$  in the case of 50 vol % DEE, but  $X_{\text{FFA}}$  is still higher in the initial stages of the reaction compared to the no co-solvent case. After 120 min of reaction,  $X_{\text{FFA}}$  was the same for both cases. This means that DEE is tolerable to the poisoning effect of water in the initial stage of reaction due to the insolubility of water into DEE. However, after 120 min, poisoning of catalyst dominates.

The comparison of acetone and DEE is depicted in Figure 5, in which 2 wt % water was added to 50 vol % of co-solvent experiments at 50 °C and 6 MR. It has been observed that

Table 3. ANOVA Table for  $X_{\text{FFA}}$  at 75 min

source	sum of squares	df	mean square	F-value	p-value
model	1099.25	9	122.14	23.36	<0.0001
A—catalyst (wt %)	590.28	1	590.28	112.89	<0.0001
B—temperature (°C)	270.53	1	270.53	51.74	<0.0001
C—co-solvent (mL/100 g of oil)	49.05	1	49.05	9.38	0.0120
AB	2.60	1	2.60	0.4973	0.4968
AC	39.15	1	39.15	7.49	0.0210
BC	16.82	1	16.82	3.22	0.1032
A <sup>2</sup>	8.55	1	8.55	1.64	0.2298
B <sup>2</sup>	48.35	1	48.35	9.25	0.0124
C <sup>2</sup>	0.7230	1	0.7230	0.1383	0.7178
residual	52.29	10	5.23		
cor total	1151.53	19			
std. dev.	2.29		R <sup>2</sup>		0.9546
mean	66.28		adjusted R <sup>2</sup>		0.9137
CV %	3.45		adeq precision		18.6762

DEE resulted in better  $X_{\text{FFA}}$  than acetone because water is soluble in acetone but not in DEE. Note that in DEE, water was present as a different phase, and due to the insolubility of water and DEE, poisoning of the catalyst is less than in acetone. Therefore, the addition of a co-solvent has intensified the esterification reaction rate in the initial stage of the reaction. Also, catalyst poisoning caused the same  $X_{\text{FFA}}$  as obtained in the no co-solvent system after 120 min of reaction. Hence, we can say that DEE is more effective in intensifying the esterification rate in comparison to acetone because DEE is found to be tolerable to water in the initial stage of the reaction, even in the presence of water.

**4.4. Effect of MR on the Amount of Co-Solvent.** Figure 6 shows the  $X_{\text{FFA}}$  at 9 MR using DEE as a co-solvent in different proportions. It can be observed from Figure 6 that  $X_{\text{FFA}}$  remained the same up to 20 vol % addition of DEE, but 30 vol % of DEE showed a significant increase in  $X_{\text{FFA}}$  in the initial period of the reaction. Further addition of DEE has a negative impact on  $X_{\text{FFA}}$ , which may be due to the dilution effect of the co-solvent.<sup>18</sup> However, after 120 min of reaction,  $X_{\text{FFA}}$  reached the same value for all the amounts of co-solvents. It can be deduced from Figures 3 and 6 that the vol % of DEE for better  $X_{\text{FFA}}$  is dependent on the MR of the methanol in the reaction system. However, the absolute amount of DEE required is identical for both 6 and 9 MR reaction, i.e., 23 mL of DEE/100 g of oil.

**4.5. Influence of Agitation Rate on Mass Transfer.** Mass transfer limitation is examined by conducting experiments at 50 °C and 6 MR for the no co-solvent system over different stirring speeds (150, 300, and 450 RPM). The results are presented in Figure S6. No considerable effect of the agitation rate on  $X_{\text{FFA}}$  was observed as there were no changes in  $X_{\text{FFA}}$  as the rate of agitation changes. If FFA is greater than 20 wt % in oil, then oil and methanol are miscible.<sup>25</sup> Similar observations are found here in the case of 50 wt % FFA so that there is no mass transfer limitation in the esterification reaction.

Furthermore, we conducted experiments at 50 °C and 6 MR for 50 vol % DEE as a co-solvent. Different agitation rates were applied, and the results are presented in Figure 7. The  $X_{\text{FFA}}$  at 150 and 300 RPM is almost the same, whereas a higher  $X_{\text{FFA}}$  was found at 450 RPM. To understand this behavior, the results of the DEE system at various RPM are compared with the results of the no co-solvent system at 450 RPM (because

the  $X_{\text{FFA}}$  at various RPM in the no co-solvent system was almost the same, see Figure S6). Figure 7 shows that in the initial periods of the reaction,  $X_{\text{FFA}}$  is higher for the DEE system compared to the no co-solvent system, even at low RPM (150 and 300). Although no mass transfer limitation is observed in the no co-solvent system (see Figure S6), there was a noticeable effect of the addition of co-solvent DEE on  $X_{\text{FFA}}$ .

#### 4.6. Continuous Removal of Water Using Molecular Sieves as Adsorbents.

**4.6.1. Co-Solvent Acetone.** To observe the effects of water adsorption on  $X_{\text{FFA}}$ , experiments are conducted at 9 MR and 60 °C reaction temperature, using molecular sieves as adsorbents at total reflux conditions. The effect of water removal on  $X_{\text{FFA}}$  in the acetone system is examined because water is soluble in acetone. The experiment is started at 9 MR and 60 °C, using 75 mL of acetone as co-solvent, under total reflux conditions. It is observed that the amount of acetone is not sufficient as no significant vapors were formed. Therefore, 100, 150, and 200 mL of acetone were taken, while the experiments setups were the same (at 9 MR and 60 °C), and the results are shown in Figure 8. It can be observed from Figure 8 that 100 mL of acetone resulted in higher  $X_{\text{FFA}}$  in comparison to 150 and 200 mL of acetone used at the same reaction conditions in the initial stage of the reaction. This negative effect of a high amount of acetone on  $X_{\text{FFA}}$  can be due to the dilution effect of co-solvents.<sup>18</sup> After 120 min,  $X_{\text{FFA}}$  reached the same value (~94%) for all the amounts of acetone. Equilibrium  $X_{\text{FFA}}$  for 9 MR and 60 °C reaction conditions is calculated from a previous work<sup>26</sup> and found to be around 93.9%, equal to the maximum  $X_{\text{FFA}}$  obtained for the acetone system, as shown in Figure 9.

Results are compared with the system without adsorption at the same reaction condition, and the results are presented in Figure 9.  $X_{\text{FFA}}$  was slightly higher in the initial period in the case of no co-solvent in comparison to the co-solvent systems (with adsorption and without adsorption). This is due to dilution at 100 mL of acetone. However, after 45 min of reaction,  $X_{\text{FFA}}$  reached the same value for all systems and this could be explained by the poisoning effect of water on the sulfuric acid catalyst.<sup>27</sup> The co-solvent with adsorption resulted in the same  $X_{\text{FFA}}$  as in the co-solvent without adsorption. Even though MR of methanol was less than 9 MR in the adsorption system since methanol as vapor is also present in the condenser and flask (containing molecular sieves), under

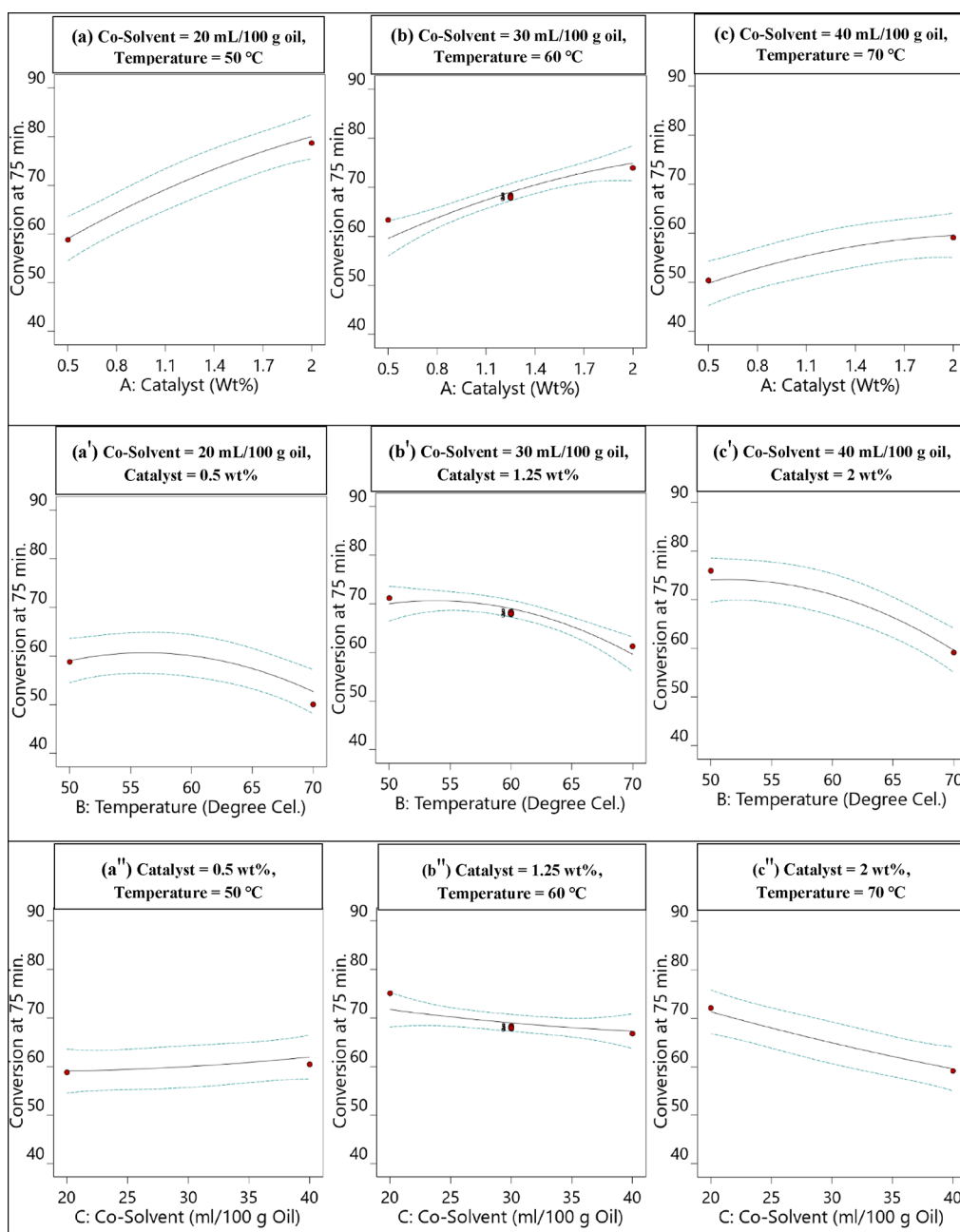


**Figure 12.** Main effect plots: (a, b, c) for catalyst, (a', b', c') for temperature, and (a'', b'', c'') for co-solvent (a, a', a'': low level, b, b', b'': middle level, and c, c', c'': higher level), at 75 min  $X_{FFA}$ .

total reflux conditions, this means that the effect of water adsorption on  $X_{FFA}$  is positive. However,  $X_{FFA}$  is much higher than the  $X_{FFA}$  obtained in the co-solvent without an adsorption system. Hence, we can say that acetone is not suitable for effective water removal and it is recommended to study DEE as a co-solvent for effective water removal.

Furthermore, DEE is nonpolar in nature and can act as an inert co-solvent that generates an oil-rich single-phase system so that all reactions are taking place in the same phase, allowing better contact between the reactants and hence faster reactions. It is also used as an ignition improver in the combustion engine. Owing to all these properties of DEE, DEE is also selected as an entrainer for the continuous removal of water under low-temperature operating conditions in this study.

**4.6.2. Co-Solvent DEE.** Figure 10 shows the effect of DEE at 50 °C and 6 MR when the DEE amount is 49 mL (50%). The results are compared with the experiment without a co-solvent. The addition of DEE has slightly increased  $X_{FFA}$ . However, fewer vapors in the condenser were observed. Sufficient vapors are achieved at 144 mL in case of adsorption, but the addition of DEE has a negative impact on  $X_{FFA}$ , which may be due to the dilution effect of the co-solvent.

In Figure 11, we present the effect of DEE at 60 °C with sufficient vapors produced by 69 mL of DEE. The results are compared with the experiment without a co-solvent. The addition of DEE has a negative impact on  $X_{FFA}$ , which may be due to the dilution effect of the co-solvent at 60 °C. Therefore, removing water at a low temperature is not applicable and could be achieved with another entrainer. Hence, using the

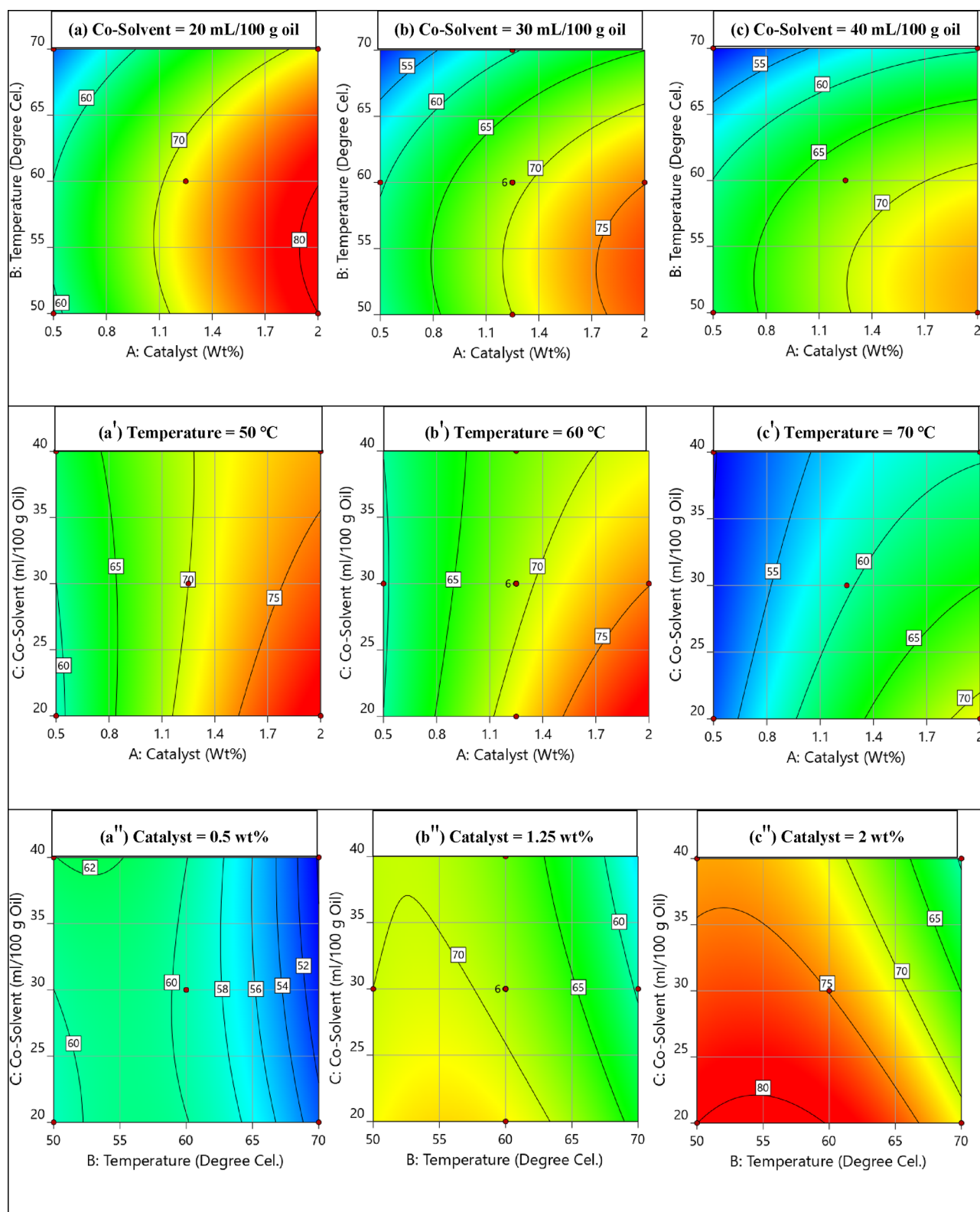


**Figure 13.** Contour plots: (a, b, c) for co-solvent, (a', b', c') for temperature and (a'', b'', c''), for catalyst (a, a', a'': low level, b, b', b'': middle level, and c, c', c'': higher level) at 75 min  $X_{\text{FFA}}$ .

molecular sieves with acetone and DEE as entrainers is not feasible for removing the water at low temperatures. It is required to complete the reaction within 75 min before the starting of poisoning on the sulfuric acid catalyst, as discussed before.

**4.7. Optimization of the Process.** The  $X_{\text{FFA}}$  percentage at 10, 20, 30, 45, and 75 min in Table S2 is treated as the response factor. The statistical software Design-Expert (12th version) is used to analyze results, regression models, and optimization interpretation.



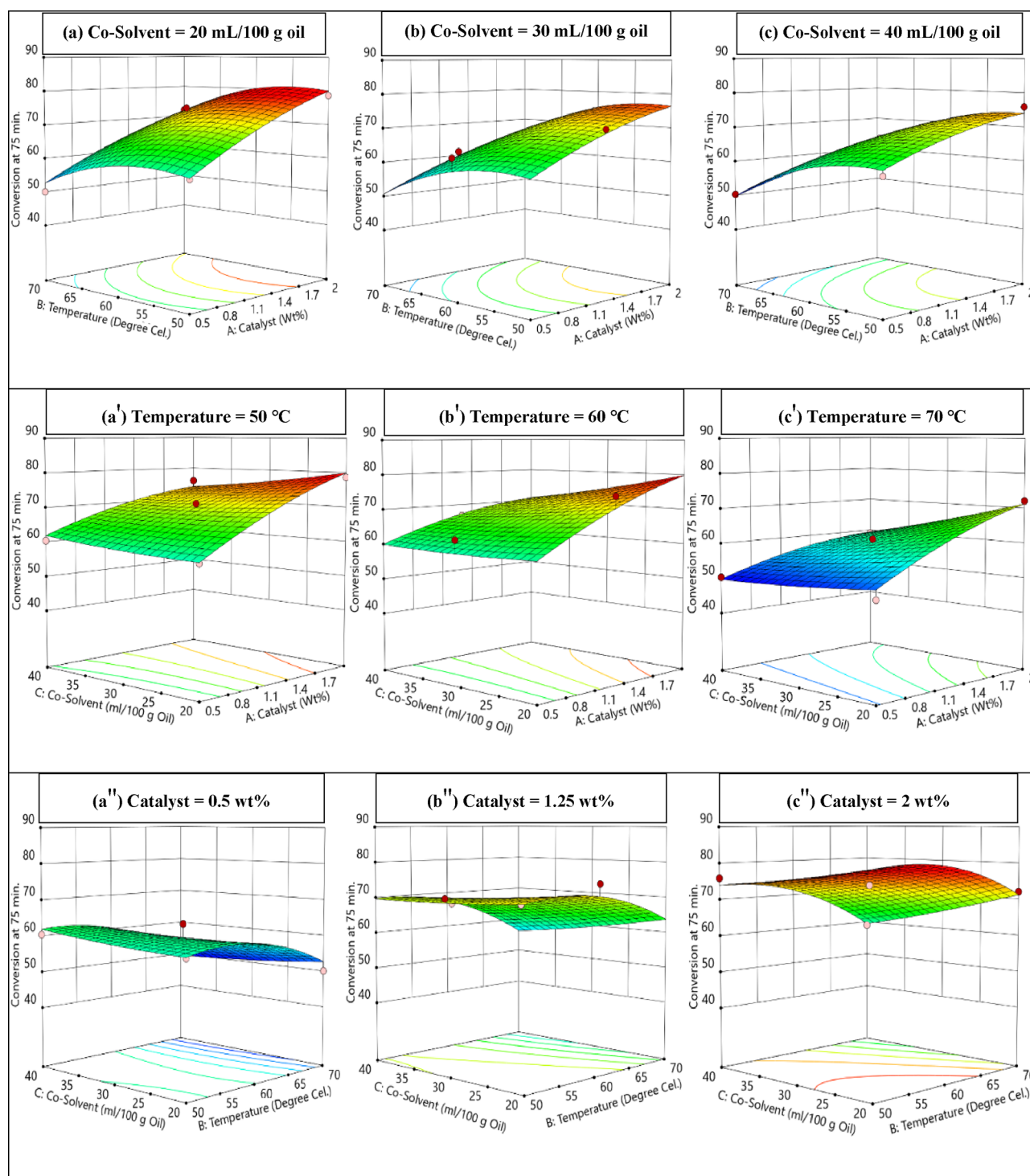


**Figure 14.** Surface plots: (a, b, c) for co-solvent, (a', b', c') for temperature and (a'', b'', c''), for catalyst (a, a', a'': low level, b, b', b'': middle level, and c, c', c'': higher level) at 75 min  $X_{FFA}$ .

**4.7.1. Analysis of Variance (ANOVA).** Complete ANOVA tables at 10, 20, 30, 45, and 75 min are presented in Tables S3, S4, S5, and S6 and Table 3, respectively. Catalyst, temperature, and co-solvent were denoted as A, B, and C, respectively. The model  $F$ -values at 10, 20, 30, 45, and 75 min imply that the model is significant. At a 95% confidence level,  $p$ -values less than 0.05 indicate that the model terms are significant and those greater than 0.05 are not significant model terms. A, B, and C are significant model terms at 10, 20, 30, 45, and 75 min

cases. Adeq precision measures the signal-to-noise ratio. A ratio greater than 4 is desirable; all the ratios at 10, 20, 30, 45, and 75 min cases are more significant than 4 and indicate an adequate signal. Therefore, these models can be used to navigate the design space.

All the parameters and some of their interactions and curvature effects are inferred to be significant for the intensification of the esterification reaction. Therefore, the

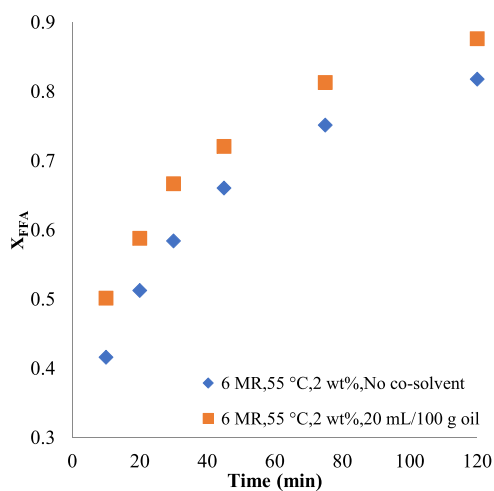


Figure 15. Effect of optimized co-solvent on  $X_{\text{FFA}}$ .

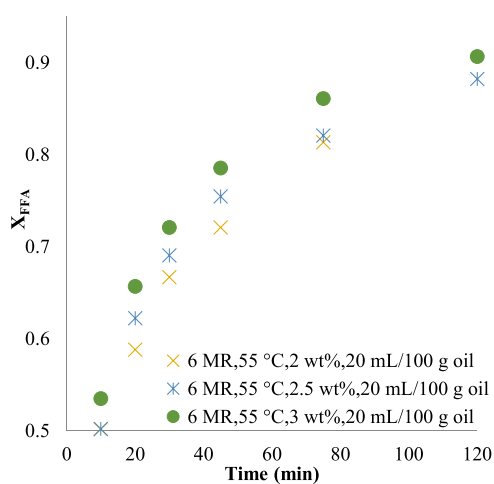


Figure 16. Effect of optimized catalyst on  $X_{\text{FFA}}$ .

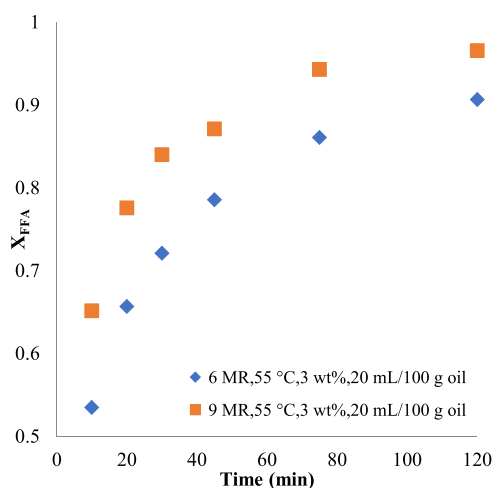


Figure 17. Effect of optimized MR on  $X_{\text{FFA}}$ .

main effects, interaction, and curvature effects of parameters are discussed below.

**4.7.2. Main and Curvature Effect Plots.** Figures S7, S8, S9, and S10 and Figure 12 illustrate the effect of catalyst (wt %), temperature (°C), and co-solvent (mL/100 g of oil) on  $X_{\text{FFA}}$  at 10, 20, 30, 45, and 75 min.

Catalyst amount plays a substantial role in efficient  $X_{\text{FFA}}$ . Throughout the reaction,  $X_{\text{FFA}}$  linearly increased with increasing catalyst amount due to its acid strength, which is responsible for releasing more  $\text{H}^+$  species to protonate the carboxylic moiety of the fatty acid (rate determinant step).<sup>28–30</sup>

Raising the reaction temperature in the range of 50 to 70 °C resulted in a nonlinear behavior on  $X_{\text{FFA}}$  (at low- and middle-level settings). Operating in the range of 50 to 60 °C has improved the  $X_{\text{FFA}}$  throughout the reaction time. Raising the reaction temperature up to 70 °C resulted in a decrease in  $X_{\text{FFA}}$  throughout the reaction time. By operating in the range of 50 to 55 °C,  $X_{\text{FFA}}$  increased in the case of a high-level setting throughout the reaction time but a further rise in reaction temperature resulted in a decrease in  $X_{\text{FFA}}$ ; this might be due to the presence of more methanol and co-solvent as vapors in the condenser.<sup>31</sup> Therefore, the maximum  $X_{\text{FFA}}$  could be achieved in the range of 50 to 55 °C. Also, Wei et al.<sup>32</sup> stated that, by operating in a microwave reactor, the deacidification rate (DR) reached 90.80% when the temperature was elevated from 55 to 65 °C. However, DR decreased when the reaction temperature was above 65 °C.

By increasing the co-solvent (DEE) amount to more than 20 mL/100 g of oil,  $X_{\text{FFA}}$  linearly decreased at low, middle, and high levels throughout the reaction time due to dilution. Therefore, the maximum  $X_{\text{FFA}}$  achieved 20 mL/100 g of oil.

**4.7.3. Contour Plots and Surface Plots.** The contour plots and surface plots represented from Figures S11–S18 and Figures 13 and 14 showed the effect of experimental factors (catalyst, temperature, and co-solvent) at lower, middle, and higher settings for 10, 20, 30, 45, and 75 min  $X_{\text{FFA}}$ . The maximum  $X_{\text{FFA}}$  (>80%) could be achieved at a low-level-setting co-solvent amount, i.e., 20 mL/100 g of oil. Any further addition of co-solvent resulted in the negative effect of the  $X_{\text{FFA}}$  dilution effect. Initially, the increase in  $X_{\text{FFA}}$  is due to the increased contact area between methanol and oil and the increased mutual solubility in the presence of a co-solvent. Later, the excess co-solvent started to affect the contact between the reactants due to excess increased insolubility, which resulted in lower  $X_{\text{FFA}}$  after the addition of more than 20 mL/100 g of oil co-solvent. The maximum  $X_{\text{FFA}}$  (>75%) could be achieved in the range from 50 to 55 °C. A further increase in temperature resulted in a negative effect on  $X_{\text{FFA}}$ . This might be due to the presence of methanol and co-solvent as vapors in the condenser, and hence the MR and co-solvent are not as calculated in the reaction medium. Therefore, the maximum  $X_{\text{FFA}}$  could be achieved in the range of 50 to 55 °C. For the high-level-setting wt % catalyst, i.e., 2 wt %, a maximum  $X_{\text{FFA}}$  (>80%) could be achieved because of the high tolerance to water poisoning. Also, decreasing the catalyst wt % resulted in a decrease of  $X_{\text{FFA}}$ . Acid strength is responsible for releasing more  $\text{H}^+$  species to protonate the carboxylic moiety of the fatty acid (rate determinant step).<sup>28–30</sup>

Hence, there is a range of variation in the effect of the parameters and it is required to optimize these ranges to achieve the maximum  $X_{\text{FFA}}$  within 75 min.

**4.7.4. Optimization of Parameters.** Contour plots and surface plots showed a maximum  $X_{\text{FFA}}$  at 55 °C, 20 mL/100 g of oil co-solvent, and 2 wt % catalyst. At these conditions (55 °C, 20 mL/100 g of oil co-solvent, and 2 wt % catalyst), the experiment was performed and the  $X_{\text{FFA}}$  achieved was equal to 81.33% within 75 min, as shown in Figure 15. To show the significance of a co-solvent system over the no co-solvent

system, we compared the results of both systems at the same operating conditions in Figure 15. The highest  $X_{\text{FFA}}$  achieved in the case of a no co-solvent system was 75.18% within 75 min, while it was 81.33% within 75 min in the case of a co-solvent system. The present study aims to optimize the parameters for the intensification of esterification reaction and minimize the percentage of FFA. It is required to operate at 55 °C and increase the MR up to 9 and catalyst up to 3 wt % so that the  $X_{\text{FFA}}$  will increase more than 90%, as discussed below.

The results of increasing the catalyst beyond 2 wt % at 55 °C, 6 MR, and 20 mL/100 g of oil co-solvent are shown in Figure 16. It was observed that  $X_{\text{FFA}}$  increased from 81.33 to 86.08%, while the catalyst increased from 2 to 3 wt %. Since the vol % of DEE for better  $X_{\text{FFA}}$  is dependent on the MR of the methanol in the reaction system (see Section 4.4), we increased the MR from 6 to 9 at 55 °C, 3 wt % catalyst, and 20 mL/100 g of oil co-solvent; the results are shown in Figure 17.  $X_{\text{FFA}}$  increased from 86.08 to 94.29% within 75 min. Therefore, we can state that 55 °C, 9 MR, 3 wt %, and 20 mL/100 g of oil co-solvent are the optimized operating conditions to achieve a high  $X_{\text{FFA}}$  of up to 95%.

## 5. CONCLUSIONS

The present study focused on developing and optimizing a low-temperature intensification process to enhance the biodiesel yield and reduce energy consumption. An optimized co-solvent amount without an adsorption system is found to be better than the conventional system to obtain a high  $X_{\text{FFA}}$  at lower operating temperatures. When DEE was used as a co-solvent,  $X_{\text{FFA}}$  reached up to 95% within 75 min at 20 mL/100 g of oil DEE, 9 MR, 3 wt %  $\text{H}_2\text{SO}_4$ , and 55 °C at 320–350 RPM.

## ■ ASSOCIATED CONTENT

### SI Supporting Information

The Supporting Information is available free of charge at <https://pubs.acs.org/doi/10.1021/acsomega.3c02434>.

Miscibility chart for various co-solvents;  $X_{\text{FFA}}$  at different times; ANOVA table for  $X_{\text{FFA}}$  at 10 min; ANOVA table for  $X_{\text{FFA}}$  at 20 min; ANOVA table for  $X_{\text{FFA}}$  at 30 min; ANOVA table for  $X_{\text{FFA}}$  at 45 min; effect of MR at 40 °C; effect of temperature at 9 MR; effects of acetone added in different vol % at 50 °C and 6 MR; 50 vol % acetone system: effect of water at 6 MR and 50 °C; 50 vol % DEE system: effect of water at 6 MR and 50 °C; no co-solvent system: effect of agitation rate on  $X_{\text{FFA}}$  at 50 °C and 6 MR; main effect plots; contour plots; surface plots (PDF)

## ■ AUTHOR INFORMATION

### Corresponding Author

Alaaddin M. M. Saeed – UNILAB, State Key Laboratory of Chemical Engineering, East China University of Science and Technology, Shanghai 200237, China; Department of Petroleum Studies, Zakir Husain College of Engineering and Technology, Faculty of Engineering and Technology, Aligarh Muslim University, Aligarh 202002, India; [orcid.org/0000-0001-8772-4754](https://orcid.org/0000-0001-8772-4754); Email: [saeedalaaddin@gmail.com](mailto:saeedalaaddin@gmail.com)

### Authors

Shivika Sharma – Department of Petroleum Studies, Zakir Husain College of Engineering and Technology, Faculty of

Engineering and Technology, Aligarh Muslim University, Aligarh 202002, India

Saeikh Zaffar Hassan – Department of Petroleum Studies, Zakir Husain College of Engineering and Technology, Faculty of Engineering and Technology, Aligarh Muslim University, Aligarh 202002, India

Atef M. Ghaleb – Department of Industrial Engineering, College of Engineering, Alfaisal University, 11533 Riyadh, Saudi Arabia

Gui-Ping Cao – UNILAB, State Key Laboratory of Chemical Engineering, East China University of Science and Technology, Shanghai 200237, China

Complete contact information is available at:

<https://pubs.acs.org/10.1021/acsomega.3c02434>

## Notes

The authors declare no competing financial interest.

## ■ ACKNOWLEDGMENTS

The authors would like to thank Aligarh Muslim University, East China University of Science and Technology, and Alfaisal University for the necessary support for this research work.

## ■ REFERENCES

- (1) Abidin, S. Z.; Haigh, K. F.; Saha, B. Esterification of Free Fatty Acids in Used Cooking Oil Using Ion-Exchange Resins as Catalysts: An Efficient Pretreatment Method for Biodiesel Feedstock. *Ind. Eng. Chem. Res.* **2012**, *51*, 14653–14664.
- (2) Dharma, S.; Ong, H. C.; Masjuki, H. H.; Sebayang, A. H.; Silitonga, A. S. An overview of engine durability and compatibility using biodiesel–bioethanol–diesel blends in compression-ignition engines. *Energy Convers. Manage.* **2016**, *128*, 66–81.
- (3) Lucena, I. L.; Saboya, R. M. A.; Oliveira, J. F. G.; Rodrigues, M. L.; Torres, A. E. B.; Cavalcante, C. L., Jr.; Parente, E. J. S., Jr.; Silva, G. F.; Fernandes, F. A. N. Oleic acid esterification with ethanol under continuous water removal conditions. *Fuel* **2011**, *90*, 902–904.
- (4) Chuah, L. F.; Klemeš, J. J.; Bokhari, A.; Asif, S. A Review of Biodiesel Production from Renewable Resources: Chemical Reactions. *Chem. Eng. Trans.* **2021**, *88*, 943–948.
- (5) Chuah, L. F.; Klemeš, J. J.; Bokhari, A.; Asif, S.; Cheng, Y. W.; Chong, C. C.; Show, P. L. A review of intensification technologies for biodiesel production. In *Biofuels and Biorefining*; Gutiérrez-Antoni, C.; Gómez Castro, F. I. Eds.; Elsevier, 2022; pp. 87–116, DOI: 10.1016/B978-0-12-824117-2.00009-0.
- (6) Demirbas, A.; Bafail, A.; Ahmad, W.; Sheikh, M. Biodiesel production from non-edible plant oils. *Energy Explor. Exploit.* **2016**, *34*, 290–318.
- (7) Joshi, S. M.; Gogate, P. R.; Suresh Kumar, S. Intensification of esterification of karanja oil for production of biodiesel using ultrasound assisted approach with optimization using response surface methodology. *Chem. Eng. Process.* **2018**, *124*, 186–198.
- (8) Bokhari, A.; Yusup, S.; Asif, S.; Chuah, L. F.; Michelle, L. Z. Y. Chapter 3 - Process intensification for the production of canola-based methyl ester via ultrasonic batch reactor: optimization and kinetic study. In *Bioreactors*; Singh, L.; Yousuf, A.; Mahapatra, D. M. Eds.; Elsevier, 2020; pp. 27–42, DOI: 10.1016/B978-0-12-821264-6.00003-6.
- (9) Hassan, S. Z.; Vinjamur, M. Parametric effects on kinetics of esterification for biodiesel production: A Taguchi approach. *Chem. Eng. Sci.* **2014**, *110*, 94–104.
- (10) Chandane, V. S.; Rathod, A. P.; Wasewar, K. L. Enhancement of esterification conversion using pervaporation membrane reactor. *Resour.-Effic. Technol.* **2016**, *2*, S47–S52.
- (11) Jeong, J. C.; Lee, S. B. Enzymatic esterification reaction in organic media with continuous water stripping: effect of water content

on reactor performance and enzyme agglomeration. *Biotechnol. Tech.* **1997**, *11*, 853–858.

(12) Pradana, Y. S.; Hidayat, A.; Prasetya, A.; Budiman, A. Biodiesel production in a reactive distillation column catalyzed by heterogeneous potassium catalyst. *Energy Procedia* **2017**, *143*, 742–747.

(13) Rastegari, H.; Ghaziaskar, H. S.; Yalpani, M.; Shafiei, A. Development of a Continuous System Based on Azeotropic Reactive Distillation to Enhance Triacetin Selectivity in Glycerol Esterification with Acetic Acid. *Energy Fuels* **2017**, *31*, 8256–8262.

(14) Nijhuis, T. A.; Beers, A. E. W.; Kapteijn, F.; Moulijn, J. A. Water removal by reactive stripping for a solid-acid catalyzed esterification in a monolithic reactor. *Chem. Eng. Sci.* **2002**, *57*, 1627–1632.

(15) Lucena, I. L.; Silva, G. F.; Fernandes, F. A. N. Biodiesel Production by Esterification of Oleic Acid with Methanol Using a Water Adsorption Apparatus. *Ind. Eng. Chem. Res.* **2008**, *47*, 6885–6889.

(16) Singh, V.; Yadav, M.; Sharma, Y. C. Effect of co-solvent on biodiesel production using calcium aluminium oxide as a reusable catalyst and waste vegetable oil. *Fuel* **2017**, *203*, 360–369.

(17) Zhou, H.; Lu, A.; Liang, B. Solubility of Multicomponent Systems in the Biodiesel Production by Transesterification of *Jatropha curcas* L. Oil with Methanol. *J. Chem. Eng. Data* **2006**, *51*, 1130–1135.

(18) Lee, M.-J.; Kuoa, Y.-C.; Lienb, P.-J.; Lina, H.-M. Liquid-Liquid Equilibria for Ternary Mixtures Containing Vegetable Oils, Methanol, and Cosolvents. *Open Thermodyn. J.* **2010**, *4*, 122–128.

(19) Guan, G.; Sakurai, N.; Kusakabe, K. Synthesis of biodiesel from sunflower oil at room temperature in the presence of various cosolvents. *Chem. Eng. J.* **2009**, *146*, 302–306.

(20) Encinar, J. M.; Pardal, A.; Sánchez, N. An improvement to the transesterification process by the use of co-solvents to produce biodiesel. *Fuel* **2016**, *166*, 51–58.

(21) Maeda, Y.; Thanh, L. T.; Imamura, K.; Izutani, K.; Okitsu, K.; Boi, L. V.; Ngoc Lan, P.; Tuan, N. C.; Yoo, Y. E.; Takenaka, N. New technology for the production of biodiesel fuel. *Green Chem.* **2011**, *13*, 1124–1128.

(22) Qu, Y.; Peng, S.; Wang, S.; Zhang, Z.; Wang, J. Kinetic Study of Esterification of Lactic Acid with Isobutanol and n-Butanol Catalyzed by Ion-exchange Resins. *Chin. J. Chem. Eng.* **2009**, *17*, 773–780.

(23) Yadav, G. D.; Pawar, S. V. Synergism between microwave irradiation and enzyme catalysis in transesterification of ethyl-3-phenylpropanoate with n-butanol. *Bioresour. Technol.* **2012**, *109*, 1–6.

(24) Chuah, L. F.; Klemesš, J. J.; Yusup, S.; Bokhari, A.; Akbar, M. M.; Chong, Z. K. Kinetic studies on waste cooking oil into biodiesel via hydrodynamic cavitation. *J. Cleaner Prod.* **2017**, *146*, 47–56.

(25) Liu, Y.; Lu, H.; Liu, C.; Liang, B. Solubility Measurement for the Reaction Systems in Pre-Esterification of High Acid Value *Jatropha curcas* L. Oil. *J. Chem. Eng. Data* **2009**, *54*, 1421–1425.

(26) Hassan, S. Z.; Vinjamur, M. Analysis of Sensitivity of Equilibrium Constant to Reaction Conditions for Esterification of Fatty Acids with Alcohols. *Ind. Eng. Chem. Res.* **2013**, *52*, 1205–1215.

(27) Bokhari, A.; Chuah, L. F.; Yan Michelle, L. Z.; Asif, S.; Shahbaz, M.; Akbar, M. M.; Inayat, A.; Jamil, F.; Naqvi, S. R.; Yusup, S. Microwave enhanced catalytic conversion of canola-based methyl ester. In *Advanced Biofuels*; Azad, A. K.; Rasul, M. Eds.; Woodhead Publishing, 2019; pp. 153–166, DOI: 10.1016/B978-0-08-102791-2.00006-4.

(28) Aranda, D. A. G.; Santos, R. T. P.; Tapanes, N. C. O.; Ramos, A. L. D.; Antunes, O. A. C. Acid-Catalyzed Homogeneous Esterification Reaction for Biodiesel Production from Palm Fatty Acids. *Catal. Lett.* **2008**, *122*, 20–25.

(29) Patel, A.; Brahmkhatri, V. Kinetic study of oleic acid esterification over 12-tungstophosphoric acid catalyst anchored to different mesoporous silica supports. *Fuel Process. Technol.* **2013**, *113*, 141–149.

(30) Fadhil, A. B.; Aziz, A. M.; Al-Tamer, M. H. Biodiesel production from *Silybum marianum* L. seed oil with high FFA content using sulfonated carbon catalyst for esterification and base

catalyst for transesterification. *Energy Convers. Manage.* **2016**, *108*, 255–265.

(31) Asif, S.; Ahmad, M.; Bokhari, A.; Fatt, C. L.; Zafar, M.; Sultana, S.; Mir, S. Chemical Conversion in Biodiesel Refinery. In *Prospects of Renewable Bioprocessing in Future Energy Systems*; Rastegari, A. A.; Yadav, A. N.; Gupta, A. Eds.; Springer International Publishing, 2019; pp. 201–217, DOI: 10.1007/978-3-030-14463-0\_7.

(32) Lu, W.; Alam, M. A.; Wu, C.; Wang, Z.; Wei, H. Enhanced deacidification of acidic oil catalyzed by sulfonated granular activated carbon using microwave irradiation for biodiesel production. *Chem. Eng. Process.* **2019**, *135*, 168–174.